

# Influence of Electrostatic Effects on Activation Barriers in Enzymatic Reactions: Pyridoxal 5'-Phosphate-Dependent Decarboxylation of $\alpha$ -Amino Acids

Robert D. Bach,<sup>\*,1a</sup> Carlo Canepa,<sup>1b</sup> and Mikhail N. Glukhovtsev<sup>1c</sup>

Contribution from the Department of Chemistry and Biochemistry, University of Delaware, Newark, Delaware 197163

Received March 8, 1999

**Abstract:** The role of the pyridoxyl functionality on pyridoxal 5'-phosphate (PLP)-dependent enzymatic decarboxylation of  $\alpha$ -amino acids has been examined using ab initio calculations at electron-correlated levels of theory (MP2/6-31G(d) and B3LYP/6-31G(d)). The zwitterionic reactant intermediates involved are used to measure the effects of ground-state destabilization on the activation barriers. Inclusion of the 2-hydroxy-3-methylpyridine group, as in alanine imine with PLP (**5**), results in a decrease in the barrier height to 20.1 kcal/mol. Either an intramolecular 1,4-proton shift from the carboxylic acid group or general acid catalysis by the phenol group in **5** affords a protonated aldimine group that provides Coulombic stabilization for the decarboxylation step (TS-6 and TS-7). There is no change in electron density of the pyridoxyl ring in either neutral transition structure. The "electron sink" effect attributed to the amide functionality in pyruvoyl-dependent and the pyridoxyl group in PLP-dependent decarboxylation is absent. The barrier heights of the pyruvoyl-dependent (TS-3) and PLP-dependent (TS-7) decarboxylations are quite similar. The three pertinent structural features essential to efficient PLP-dependent decarboxylation are (i) the Coulombic influence of proton transfer to the imine nitrogen in the transition state for decarboxylation, (ii) the short, strong stabilizing hydrogen bond of the phenol oxygen anion with the imine hydrogen in the transition structure, and (iii) the formation of zwitterionic intermediates along the reaction coordinate with an energy-compensating Coulombic stabilization of the PLP cofactor at the active site. In decarboxylation reactions involving salt bridges, the potential for an increase in distance between oppositely charged centers must be alleviated early along the reaction coordinate by annihilation of the salt bridge to avoid marked increases in energy.

## 1. Introduction

Several theories have been put forth recently in an effort to explain the rate enhancement typically associated with enzymatic reactions relative to comparable processes that take place in solution. Considerable efforts have been expended on the question of how transition structures in these reactions may be stabilized. Electrostatic stabilization of ionic transition structures and formation of low-barrier or short, strong hydrogen bonds can be considered as two main factors that can influence reaction barriers. The first of these has been discussed by Warshel, who advocated that enzymes function by solvation substitution at the active site.<sup>2</sup> He suggests that enzymes work by modulating the difference between the electrostatic energies of the transition structure (TS) and the ground state (GS). The catalytic effect of the enzyme is then essentially the difference in stabilization energies of the relevant state in the enzyme and in the corresponding reference solvent system. Within this context,

electrostatic solvation of ionic TS is clearly one of the most important aspects of enzyme catalysis.

It has also been proposed recently that low-barrier hydrogen bonds (LBHBs) supply a large fraction of the energy required for transition-state stabilization.<sup>3</sup> This hypothesis involves a mechanism whereby an enzyme-bound intermediate or transition state is stabilized by the formation of a single short, strong hydrogen bond that can provide 10–20 kcal/mol of stabilization energy to the enzyme complex, resulting in a rate enhancement. Herschlag prefers to advocate the use of multiple interactions with substrate groups undergoing charge rearrangements to provide stabilization specific to the transition state.<sup>4</sup> Enzymes can use these multiple hydrogen-bonding interactions, where each makes a modest energetic contribution, in a nonaqueous environment. While none of these theories is without detractors<sup>5</sup> and there is yet to be a consensus on how the stabilization is provided,<sup>2</sup> there is little question that this controversy has enhanced our understanding of enzymatic catalysis.

(1) (a) E-mail: rbach@udel.edu. WWW: <http://www.udel.edu/chem/bach>. (b) Present address: Dipartimento di Chimica Generale e Organica Applicata Corso Massimo d'Azeglio, 48, 10125 Torino, Italy. (c) E-mail: mng@udel.edu. WWW: <http://udel.edu/~mng>.

(2) (a) Warshel, A.; Aqvist, J.; Creighton, S. *Proc. Natl. Acad. Sci. U.S.A.* **1989**, *86*, 5820. (b) Warshel, A.; Papazyan, A. *Proc. Natl. Acad. Sci. U.S.A.* **1996**, *93*, 13665. (c) Warshel, A.; Aqvist, J. *Annu. Rev. Biophys. Chem.* **1991**, *20*, 267.

(3) (a) Gerlt, J. A.; Kozarich, J. W.; Keynon, G. L.; Gassman, P. G. *J. Am. Chem. Soc.* **1991**, *113*, 9667. (b) Gerlt, J. A.; Gassman, P. G. *J. Am. Chem. Soc.* **1993**, *115*, 11552. (c) Kenyon, G. L.; Gerlt, J. A.; Petsko, G. A.; Kozarich, J. W. *Acc. Chem. Res.* **1995**, *28*, 178.

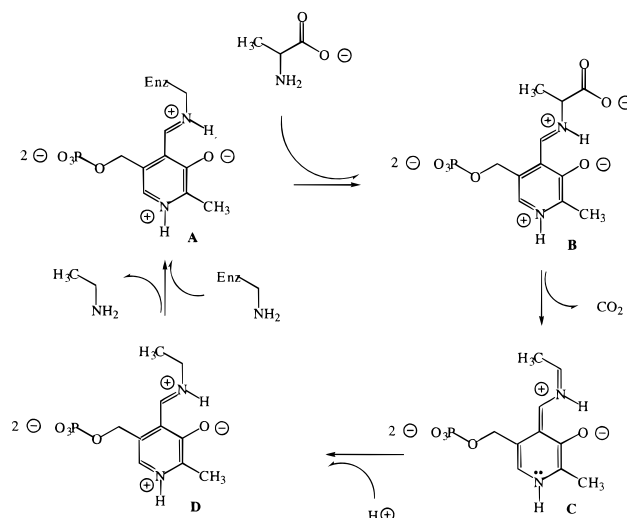
(4) (a) Shan, S.-O.; Herschlag, D. *J. Am. Chem. Soc.* **1996**, *118*, 5515. (b) Shan, S.-O.; Herschlag, D. *Proc. Natl. Acad. Sci. U.S.A.* **1996**, *93*, 14474. (c) Shan, S.-O.; Stewart, S.; Herschlag, D. *Science* **1996**, *272*, 97. (d) Narlikar, G. J.; Vidhya, G.; McConnell, T. S.; Nassim, N.; Herschlag, D. *Proc. Natl. Acad. Sci. U.S.A.* **1995**, *92*, 3668.

(5) (a) Guthrie, J. P.; Kluger, R. *J. Am. Chem. Soc.* **1993**, *115*, 11569. (b) Scheiner, S.; Tapas, K. *J. Am. Chem. Soc.* **1995**, *117*, 6970. (c) Schwartz, B.; Drueckhammer, D. G. *J. Am. Chem. Soc.* **1995**, *117*, 11902. (d) Smallwood, C. J.; McAllister, M. A. *J. Am. Chem. Soc.* **1997**, *119*, 11277. (e) Pan, Y.; McAllister, M. A. *J. Org. Chem.* **1997**, *62*, 8171.

On the other hand, there has been very little discussion concerning how the energy gap between ionic ground and transition states can be traversed in enzymatic reactions. The concept of substrate destabilization has been discussed, where the enzyme uses binding interactions with functional groups that would not otherwise interact in the GS but that do interact strongly in the TS.<sup>4d,6</sup> Gas-phase reactions forming a charged species from neutral fragments are characterized by enormous activation barriers. In the gas phase or in solution, transition state theory dictates that an ensemble of reactants will undergo many collisions until a fraction of these molecules acquires sufficient internal energy to surmount the activation barrier according to a classical picture.<sup>7</sup> How can substrates bound at the active site of a relatively immobile, high-molecular-weight enzyme, often in the virtual absence of solvent, overcome an activation barrier? In this study we examine the possible benefits of zwitterionic *destabilization* of substrate GSs and how this phenomenon can effectively lower the barrier for ionic enzymatic processes.

Pyridoxal 5'-phosphate (PLP)-dependent decarboxylation is an enzymatic reaction involving the accepted zwitterion intermediate<sup>8</sup> that can serve to demonstrate the advantageous effects of both electrostatic stabilization of the TS and destabilization of the GS on the overall reaction barrier. Enzymatic decarboxylation processes involving  $\alpha$ -amino acids constitute an important class of biochemical reactions.<sup>9</sup> This decarboxylation reaction is a key step in the synthesis of neurotransmitter amino compounds.<sup>9</sup> Mechanistic studies on the enzymatic decarboxylation of  $\alpha$ -amino acids have typically been aimed at the identification of the key reaction intermediates. Such enzymes are known to form intermediate imino compounds by exchange between the amino group of the  $\alpha$ -amino acid and the imine functionality of the enzyme prosthetic group,<sup>9</sup> as shown in Scheme 1 for PLP-dependent enzymatic decarboxylations. Formation of quinonoid **C** from zwitterionic intermediate **B** is presumed to be facilitated by the formal deposition of the pair of electrons of the breaking C-COO<sup>-</sup> bond in consonance with the "electron sink" concept, where it is generally accepted that the PLP cofactor serves to delocalize/stabilize the developing negative charge as the carboxylate group is lost as carbon dioxide. These zwitterionic intermediates provide an ideal opportunity to examine the effects of Coulombic interactions of the functional groups involved in the mechanism of decarboxylation. We can calculate the *intrinsic* destabilization of these species in the gas phase to provide a comparison with how interactions at the active site, which has a site-specific polar environment designed for electrostatic stabilization of such ionic TS, can influence the activation barrier.

Scheme 1



Although PLP-dependent transamination and decarboxylation have been considered as one of the better understood mechanisms,<sup>8,9</sup> we suggest in this study that several conceptual aspects of these processes, including the thermodynamic driving force of the decarboxylation step, need to be reappraised. We will examine the role of the pyridoxyl functionality on PLP-dependent enzymatic decarboxylation of  $\alpha$ -amino acids. This provides an opportunity to compare pyruvate- to PLP-dependent decarboxylation at the same level of theory to ascertain if this is simply an alternate, but equally efficient, method of achieving the same objective. We also examine the more general question of how such isolated biosubstrates, localized by hydrogen bonding at an active site, acquire a sufficient increase in internal energy to overcome an activation barrier.

## 2. Methods of Calculations

Molecular orbital calculations were carried out using the Gaussian94 program system<sup>10a</sup> utilizing gradient geometry optimization.<sup>10b</sup> All structures were fully optimized at the HF, MP2, or B3LYP level of theory.<sup>11a,12</sup> The 6-31G(d) and 6-311G(d,p) basis sets<sup>11</sup> have been used throughout the study. All structures shown in Scheme 2 were fully optimized at the MP2/6-31G\* level (frozen core). Vibrational frequency calculations were used to characterize all stationary points as either minima (no imaginary frequencies) or first-order saddle points (a single imaginary frequency) at the level indicated. In general, the effect of the MP4SDTQ corrections and inclusion of diffuse functions (the 6-31+G(d) basis set) on the MP2 activation barriers for decarboxylation

(6) Jencks, W. P. *Adv. Enzymol.* **1975**, *43*, 219.

(7) Steinfeld, J. I.; Francisco, J. S.; Hase, W. L. *Chemical Kinetics and Dynamics*; Prentice Hall: Englewood Cliffs, NJ, 1989.

(8) (a) Boeker, E. A.; Snell, E. E. In *Enzymes*, 3rd ed.; Boyer, P. D., Ed.; Academic Press: New York, 1972; Vol. 6, pp 217–253. (b) Sandmaier, E.; Hale, I.; Christen, P. *Eur. J. Biochem.* **1994**, *221*, 997. (c) Gallagher, T.; Snell, E. E.; Hackert, M. L. *J. Biol. Chem.* **1984**, *264*, 12373.

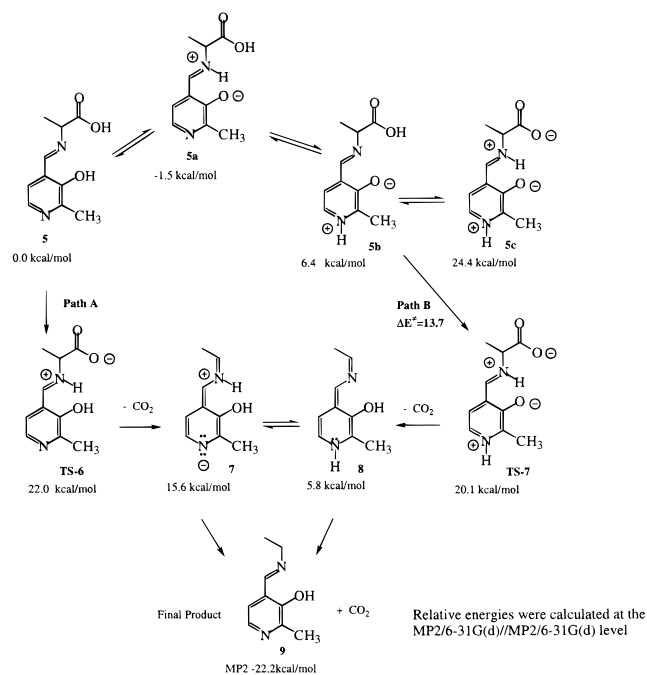
(9) (a) Lehninger, A. L.; Nelson, D. L.; Cox, M. M. *Principles of Biochemistry*; Worth Publishers: New York, 1993. (b) Walsh, C. *Enzymatic Reaction Mechanism*; W. H. Freeman and Co.: New York, 1979. (c) van Poelje, P. D.; Snell, E. E. *Annu. Rev. Biochem.* **1990**, *59*, 29. (d) Hayashi, H.; Mizuguchi, H.; Kagamiyama, H. *Biochemistry* **1993**, *32*, 812. (e) Momany, C.; Ghosh, R.; Hackert, M. *Protein Sci.* **1995**, *4*, 849. (f) Rozzell, J. H., Jr.; Benner, S. A. *J. Am. Chem. Soc.* **1984**, *106*, 4937. (g) Hohenester, E.; Keller, J. W.; Jansonius, J. N. *Biochemistry* **1994**, *33*, 13561. (h) Grishin, N. V.; Phillips, M. A.; Goldsmith, E. J. *Protein Sci.* **1995**, *4*, 1291. (i) Yoshimura, T.; Nisimura, K.; Ito, J.; Esaki, N.; Kagamiyama, H.; Manning, J. M.; Soda, K. *J. Am. Chem. Soc.* **1993**, *115*, 3897. (j) Marcus, J. P.; Dekker, E. E. *Biochem. Biophys. Res. Commun.* **1993**, *3*, 1066. (k) Graber, R.; Kasper, P.; Malashkevich, V. N.; Sandmeier, E.; Berger, P.; Gehring, J. N. J.; Christen, P. *Eur. J. Biochem.* **1995**, *232*, 686.

(10) (a) Frisch, M. J.; Trucks, G. W.; Schlegel, H. B.; Gill, P. M. W.; Johnson, B. G.; Robb, M. A.; Cheeseman, J. R.; Keith, T. A.; Peterson, G. A.; Montgomery, J. A.; Raghavachari, K.; Al-laham, M. A.; Zakrzewski, V. G.; Ortiz, J. V.; Foresman, J. B.; Cioslowski, J.; Stefanov, B. B.; Nanayakkara, A.; Challacombe, M.; Peng, C. Y.; Ayala, P. Y.; Wong, M. W.; Replogle, E. S.; Gomperts, R.; Andres, J. L.; Martin, R. L.; Fox, D. J.; Binkley, J. S.; DeFrees, D. J.; Baker, J.; Stewart, J. J. P.; Head-Gordon, M.; Gonzalez, C.; Pople, J. A. *GAUSSIAN-94*; Gaussian Inc.: Pittsburgh, PA, 1995. (b) Gonzalez, C.; Schlegel, H. B. *J. Chem. Phys.* **1989**, *90*, 2154.

(11) (a) Hehre, W. J.; Radom, L.; Schleyer, P. v. R.; Pople, J. A. *Ab Initio Molecular Orbital Theory*; Wiley: New York, 1986. (b) For Natural Population Analysis (NPA), see: (c) Reed, A. R.; Weinstock, R. B.; Weinhold, F. *J. Chem. Phys.* **1985**, *83*, 735. (d) Reed, A. E.; Curtiss, L. A.; Weinhold, F. *Chem. Rev.* **1988**, *88*, 899. (e) Weinhold, F.; Carpenter, J. E. In *The Structure of Small Molecules and Ions*; Naaman, R.; Vager, Z., Eds.; Plenum Press: New York, 1988; p 227. (f) Reed, A. E.; Weinhold, F. *Isr. J. Chem.* **1991**, *31*, 277.

(12) (a) Becke, A. D. *J. Chem. Phys.* **1993**, *98*, 5648. (b) Stevens, P. J.; Devlin, F. J.; Chablowski, C. F.; Frisch, M. J. *J. Phys. Chem.* **1994**, *80*, 11623.

## Scheme 2



of  $\beta$ -keto acids is very minimal.<sup>13a</sup> Since solvent effects play only a minor role in determining the rate for decarboxylation of  $\beta$ -keto acids, we observed excellent agreement between experiment and theory in our initial studies.<sup>13a,b</sup> Charges were calculated at the B3LYP level or using the HF wave function at the MP2/6-31G(d) geometry. The Mulliken<sup>11a</sup> and natural population (NPA)<sup>11b</sup> analyses were employed. The relatively large sizes of the molecules under consideration make calculations of charge distributions<sup>14a</sup> using the MP2 wave functions prohibitive because of their demand for computer resources.

## 3. Results and Discussion

**3.1. Assessment of the Level of Theory.** The computational ab initio study of the more complex models discussed below gives rise to considerable requirements for computer resources. As an assessment of the level of theory required to accurately describe the decarboxylation process, we computed the classical barrier for the loss of CO<sub>2</sub> from the simplest model imine derivative **1** at various computational levels. The results in Table 1 show that the Hartree–Fock (HF) decarboxylation barrier is overestimated. All three electron-correlated methods (MP2, MP4, and QCI) afford comparable results. The MP4 correlation correction on the MP2/6-31G(d) activation barrier was minimal ( $\Delta\Delta E^\ddagger = -0.6$  kcal/mol), and the QCISD(T)//QCISD/6-31G(d) barrier height ( $\Delta E^\ddagger = 31.7$  kcal/mol) differed by only 2.5 kcal/mol. The B3LYP method underestimates the barriers somewhat, as previously noted for the model pyruvoyl systems,<sup>13b</sup> but this

(13) (a) Bach, R. D.; Canepa, C. *J. Org. Chem.* **1996**, *61*, 6346. (b) Bach, R. D.; Canepa, C. *J. Am. Chem. Soc.* **1997**, *119*, 11725. (c) Bach, R. D.; Su, M.-D. *J. Am. Chem. Soc.* **1994**, *116*, 5392.

(14) (a) The Mulliken charges for **5b** calculated using the HF/6-31G(d) wave function and the MP2/6-31G(d) geometry are close to NPA charges computed using an electron-correlated (B3LYP/6-31G(d)) wave function (Figure 4). (b) The computed Mulliken or NPA charges<sup>14c</sup> on these atoms bear no resemblance to the formal charges, and, as such, formal charges should not be used to make mechanistic predictions. For example, the Mulliken and NPA charges on the pyridine nitrogen in minimum **5b** are both negative ( $-0.727$  and  $-0.470$ , respectively; the NH group charges are also negative,  $-0.300$  and  $-0.033$ ), whereas the formal charge is positive. The NPA charge on the imine nitrogen in **5a** is  $-0.560$ , and the NH group charge is  $-0.295$ . NPA charges for organic molecules generally agree with charges calculated using various schemes of population analysis.<sup>14c</sup> (c) Breneman, C. M.; Wiberg, K. B. *J. Comput. Chem.* **1990**, *11*, 361.

**Table 1.** Activation Energies (Relative to **1** in kcal/mol) for the Decarboxylation of Glycine Imine of Formaldehyde H<sub>2</sub>C=N–CH<sub>2</sub>COOH (**1**) Calculated at Various Computational Levels<sup>a</sup>

computational level	TS-2
RHF/6-31G(d)//RHF/6-31G(d)	45.8
MP2/6-31G(d)//MP2/6-31G(d)	29.8
MP4/6-31G(d)//MP2/6-31G(d)	29.2
B3LYP/6-311G(d,p)//B3LYP/6-311G(d,p)	23.8
QCISD(T)/6-31G(d)//QCISD/6-31G(d)	31.7

<sup>a</sup> The reaction is endothermic (25.9 kcal/mol at the MP2/6-31G(d) level). The calculated total energies are given in Table 1S (Supporting Information).

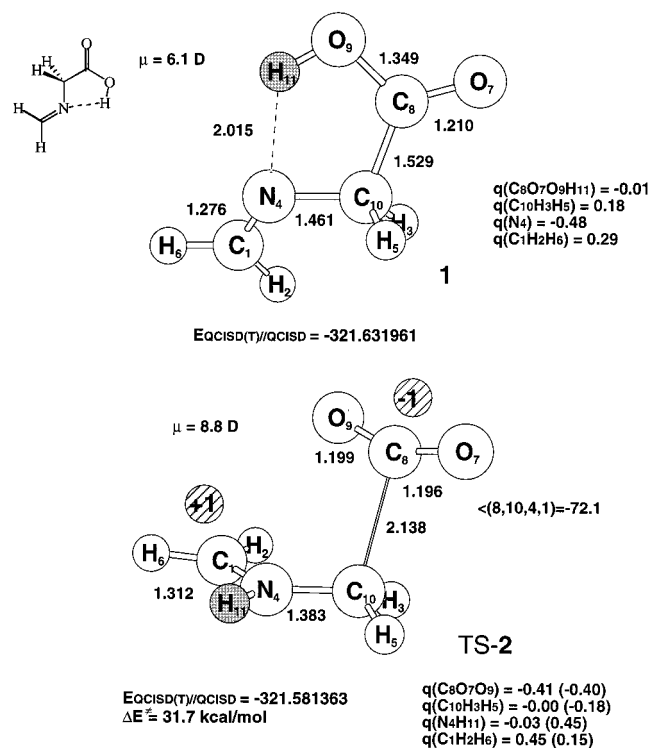


**Figure 1.** Glycine imine of formaldehyde (**1**) and its transition structure for decarboxylation (TS-2). Geometries are fully optimized at QCISD/6-31G(d). Energies are given in hartrees, distances in angstroms, and angles in degrees. Group Mulliken charges are given as  $q$ , and the net charges are in parentheses. The dipole moment  $\mu$  is given in debye.

method still provides reliable relative energetics, provided this trend is recognized. These data suggest that, while the HF level may be adequate for determining relative energies for the larger systems examined, the MP2 or a correlated level should be used to predict the activation barriers for decarboxylation.

We have examined the potential role of electron delocalization of the developing carbanionic center to an adjacent imine on the gas-phase barrier for decarboxylation.<sup>13b</sup> The MP2/6-31G(d) barrier height for decarboxylation of a simple imine derivative of glycine (**1**) (Figure 1) was predicted to be 29.8 kcal/mol. The total energies calculated at various levels of theory are listed in Table 1S (Supporting Information). In the transition structure for the decarboxylation of **1** (TS-2, Figure 1), the carboxylic acid proton is transferred to the imine nitrogen, while the C<sub>8</sub>–C<sub>10</sub>–N<sub>4</sub>–C<sub>1</sub> dihedral angle of  $-72.1^\circ$  aligns the developing electron pair, derived from the breaking C–C bond with the imine  $\pi$ -system. The relatively strong hydrogen bond between N<sub>4</sub> and H<sub>11</sub> in minimum **1** is lost in the transition structure, contributing to the relatively high barrier for decarboxylation relative to an enzymatic system. The Mulliken group charges

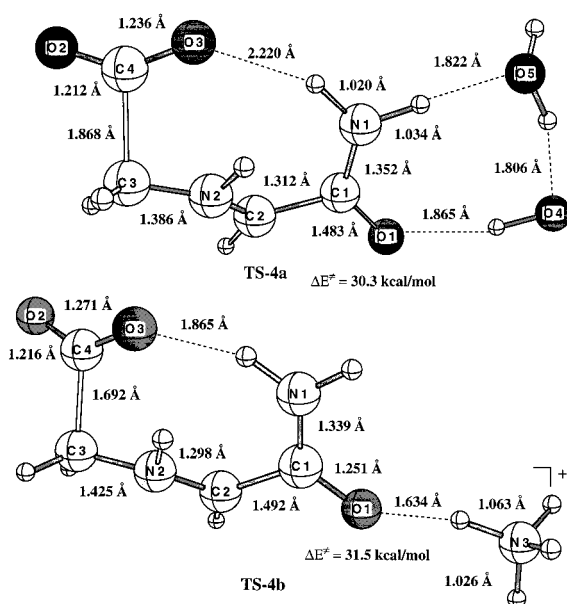
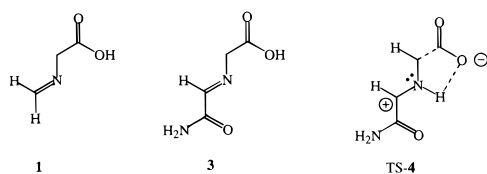


**Figure 2.** Transition structures for the decarboxylation of pyruvoyl-dependent co-factor **2** catalyzed by two water molecules (TS-4a) and an ammonium cation (TS-4b). Geometries were fully optimized at the MP2/6-31G(d) level.

given in Figure 1 indicate that the negative charge in TS-2 is on the carboxylate group ( $C_8O_7O_9$ ,  $q = -0.41$ ), while the corresponding positive center is the  $CH_2$  group ( $C_1H_2H_6$ ,  $q = 0.45$ ). The lowering of the barrier for decarboxylation of **1** ( $\Delta\Delta E^\ddagger = -35$  kcal/mol) relative to that of glycine itself<sup>13a</sup> is ascribed to electrostatic stabilization and delocalization of the charge by the  $\pi$ -system of the positively charged imine functionality. The charge on  $N_4$  in GS-1 is  $-0.48$ , while the  $N_4H_{11}$  group charge in TS-2 is close to zero ( $-0.03$ ). This approximate change in charge distribution on going from GS to TS is essentially the same for the larger PLP-containing systems and serves to demonstrate how ineffective the PLP moiety is in fulfilling its presumed role in dispersing charge in the decarboxylation process.



**3.2. Models for Enzymatic Decarboxylation.** In our first theoretical study<sup>13a</sup> on the decarboxylation process, where a variety of  $\beta$ -keto acid systems were used as models for enzymatic reactions, we provided evidence that the loss of  $CO_2$  from the simplest  $\beta$ -keto acid, formylacetic acid ( $H(C=O)CH_2COOH$ ), proceeds through a cyclic transition structure with essentially complete proton transfer from the carboxylic acid group to the  $\beta$ -carbonyl. A classical activation barrier of 28.6 kcal/mol was found for formylacetic acid, while the loss of  $CO_2$  from its corresponding carboxylate anion exhibited a reduced barrier of 20.6 kcal/mol (MP4SDTQ/6-31+G(d)//MP2/6-31+G(d)). Adjacent positively charged ammonium ions were also observed to stabilize the unimolecular loss of  $CO_2$  from a carboxylate anion by through-bond Coulombic stabilization of the transition structure. The role of electrostatic stabilization by adjacent positively charged ammonium ions in oxygen atom transfer from 4- $\alpha$ -flavin hydroperoxide has also been described recently.<sup>13c</sup>

**(a) Pyruvamide-Dependent Decarboxylase.** The above imine model system **1** was extended to include the amide functionality present in the pyruvoyl-dependent enzyme **3**. An intrinsic reaction coordinate (IRC)<sup>10b</sup> analysis established that a 1,4-proton shift from the carboxylic group to the imine nitrogen was complete before the barrier was crossed in the transition structure for decarboxylation (TS-4).<sup>13b</sup> Significantly, the  $H_2NC=O$  amide functionality in ground state (GS) model imine **3** has a group charge of 0.04, and it does not serve to disperse the developing negative charge for decarboxylation, where this group charge ( $q$ ) is actually slightly more positive in the TS ( $q(H_2NCO) = 0.07$ ). The calculated Mulliken charge distribution shows that the net charge on the  $CO_2$  fragment of TS-4 is negative ( $-0.51$ ), while the charge on the remainder of the pyruvoyl system bears an equal positive charge. The estimated barrier for the decarboxylation of isolated glycine is 64.5 kcal/mol, while that for decarboxylation of **3** is 23.1 kcal/mol (MP2/6-31G(d)). The group charge of 0.43 on the pyruvoyl C-H fragment in TS-4 shows that the positive fractional charge of the zwitterionic structure is delocalized by the  $\pi$ -system of the C=N double bond.

**(b) The Role of Hydrogen Bonding in Pyruvamide-Dependent Decarboxylation.** In this study, we also examine the potential stabilizing influence of hydrogen bonding on the calculated energetics for pyruvamide-dependent decarboxylase. When two water molecules are hydrogen bonded to the amide functionality in **3**, a hydrogen bond strength of 27.3 kcal/mol is estimated at the MP2/6-31G(d) level. The barrier height for decarboxylation (TS-4a) is reduced to 3.0 kcal/mol relative to its separated reactants but increases to 30.3 kcal/mol when measured relative to this hydrogen-bonded pre-reaction complex (Figure 2). We also included an ammonium ion ( $NH_4^+$ ) that is strongly complexed with the amide carbonyl oxygen of **2**, with a GS stabilization energy of  $-24.8$  kcal/mol. The barrier for loss of  $CO_2$  (TS-4b) relative to isolated reactants was, as anticipated<sup>13a,b</sup> for a positively charged system, also markedly reduced to 6.7 kcal/mol. However, the overall barrier for decarboxylation increased to 31.5 kcal/mol relative to this hydrogen-bonded cationic complex as a result of ground-state stabilization. As noted above,<sup>13b</sup> in the absence of catalysis, the gas-phase barrier for decarboxylation of **3** is 23.1 kcal/mol. These results do corroborate the ideas presented below, that a localized concentration of charge, either positive or negative, can markedly influence the rate of enzymatic reactions.

More importantly for the present argument, the group charge on the  $H_2N(C=O)\cdot NH_4^+$  fragment in the GS (0.96) and the TS-4b (0.99) increases slightly, supporting the idea expressed previously<sup>13b</sup> that the amide carbonyl was essentially equally polarized throughout the reaction coordinate for decarboxylation. A similar charge distribution was observed for catalysis by water, where the net charge on the  $H_2N(C=O)\cdot 2H_2O$  fragment was 0.040 in the GS and 0.064 in TS-4a. Based upon these data, we conclude that the "electron sink" effect typically attributed to the amide functionality in pyruvamide-dependent decarboxylation is not in evidence. The dominant factor in stabilizing TS-4 is the Coulombic stabilization afforded by the adjacent positively charged iminium ion functionality. The destabilization energy associated with ionic species in the gas phase is large, but the zwitterionic species involved in decarboxylation can be stabilized by the surrounding protein environment in an enzymatic reaction. If both the GS and the TS are stabilized to the same extent, i.e., if the zwitterionic TS closely resembles the GS, then the theoretically derived classical

activation barriers can provide a reasonable estimate of the energetics of the enzymatic system.<sup>8b</sup>

**3.3. Model Pyridoxal 5'-Phosphate.** In enzymatic catalysis, the binding energy from noncovalent secondary interactions is used to arrange the active site in the folded protein. The prepositioning of the hydrogen bond acceptors with respect to the hydrogen bond donors minimizes the entropic penalty that must be paid in order to bind and properly orient the substrate with respect to the catalytic groups.<sup>4</sup> Due to the zwitterionic nature of the substrate, both the GS and the TS should be stabilized by hydrogen-bonding interactions with amino acid residues at the active site. Analysis of the overall reaction energetics must take into account the energy of the GS, and the overall energy of the TS must be measured relative to the GS irrespective of any gas-phase intermediates that may lie on the reaction pathway. If the GS stabilization energy is greater than that of the TS, the energy gap between them widens, and the activation energy for the decarboxylation reaction can become excessive.<sup>13b</sup> Although zwitterionic intermediates typically exhibit an increase in energy in the gas phase (Scheme 2), the increased secondary bonding of these dipolar species with residues at the active site can effectively lower their energy while maintaining the essential zwitterionic structural features required for efficient decarboxylation. It is also quite possible that energetically favorable site-specific Coulombic interactions of the PLP cofactor with amino acid residues could result in a zwitterionic GS in much the same fashion that amino acids exist as zwitterions in polar media. With this caveat in mind, we will provide the intrinsic gas-phase barriers that we compute in the absence of solvent but also attempt to predict the influence of the interactions at the active site upon the overall energetics.

To assess the role of electron delocalization and electrostatic interactions on the barrier for decarboxylation in PLP-dependent decarboxylation, we have extended model imine **1** to include a pyridoxal ring. It has been suggested that the developing negative charge on the  $\alpha$ -carbon of the amino acid is dispersed via the  $\pi$ -system of the coenzyme, as proposed in Scheme 1.<sup>9</sup> The terminal methylene group of **1** was substituted with the 2-hydroxy-3-methylpyridine group as in **5** (Scheme 2). The phosphate group has been omitted on the grounds that it should not have a major effect upon the electron distribution. Although this negatively charged fragment could exert a Coulombic influence on the adjacent iminium ion, there is no direct resonance interaction with the ring because it is linked to the pyridoxyl ring through a  $\text{CH}_2$  group, and thus this electronic effect should be the same in both the zwitterionic GS and TS.

**(a) The Effect of Charge Separation on the Energy of the Reactant Ground State.** Since a separation in charge is typically associated with an increase in energy, we examined the relative energies of the zwitterionic structures that have been proposed for PLP systems.<sup>8,9</sup> The proton distribution of the phenolic, carboxylic acid, and basic nitrogen functionalities is usually based upon their corresponding  $\text{pK}_a$  values in water. The relative energies for MP2/6-31G(d) geometry optimizations on various minima and transition structures with different proton distributions are shown in Scheme 2. Proton transfer from the phenolic group in **5** ( $\mu = 5.8$  D, Figure 4) to the imine nitrogen, affording minimum **5a**, having the lowest dipole moment ( $\mu = 4.8$  D, Figure 4), is associated with a small decrease in energy (1.5 kcal/mol; 5.2 kcal/mol at the B3LYP/6-31G(d) level). The actual change in the calculated charge on the oxygen and nitrogen atoms is minimal,<sup>14</sup> and the strong intramolecular  $\text{O}\cdots\text{H}$  hydrogen bond in **5a**, where the  $\text{O}\cdots\text{H}$  bond distance is 1.674 Å (Figure 4), contributes to the lower energy. The  $\text{C}_{10}$ –

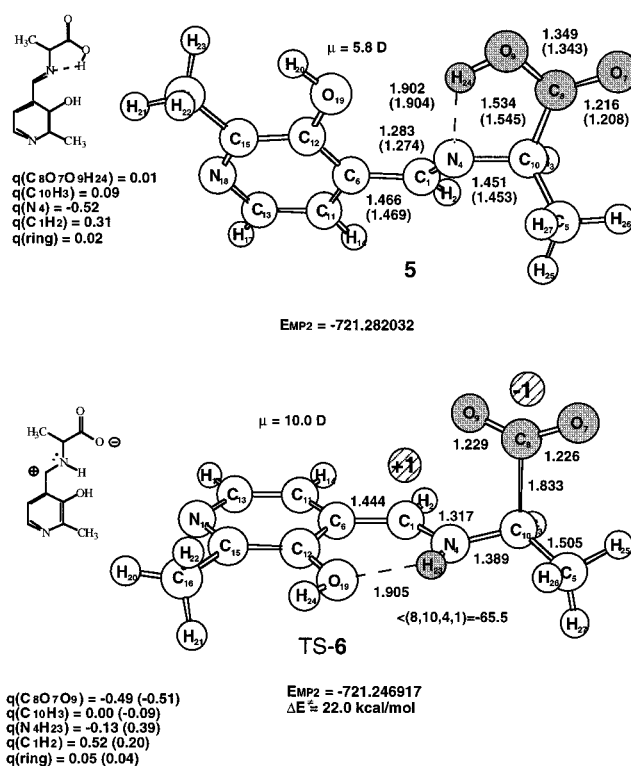


**Figure 3.** Alanine imine with PLP (**5**) and its transition structure for decarboxylation (TS-6). Geometries are fully optimized at MP2/6-31G(d). Energies are given in hartrees, distances in angstroms, and angles in degrees. Group Mulliken charges are given as  $q$ , and the net changes are in parentheses. Geometrical parameters for **5** optimized at the B3LYP level are given in parentheses.

$\text{C}_8$  bond length is shortened by 0.015 Å in **5a** with respect to that in **5** and slightly elongated (to 1.540 Å, MP2/6-31G(d)) in **5b** (Figures 3 and 4).

The charges depicted in minimum **5a** (Scheme 2) are formal charges, and the calculated Mulliken negative charge on the imine nitrogen in **5** (−0.52) actually increases (in absolute value) in zwitterionic minimum **5a** (−0.76), whereas the formal charge on the nitrogen is +1. When the formal charges in **5** are due to a transfer of the phenolic hydrogen to the pyridine nitrogen, as in zwitterionic structure **5b** ( $\mu = 13.8$  D, Figure 4),<sup>14a</sup> the energy difference increases to 6.4 kcal/mol (6.5 kcal/mol at the B3LYP/6-31G(d) level, see Table 3S, Supporting Information) as a consequence of the increase in charge separation. The NPA charges calculated for **5a** and **5b** at the B3LYP level agree with the Mulliken charges computed using the HF wave functions at the MP2/6-31G(d) geometry (Figure 4). While the 2-hydroxy-3-methylpyridine moiety in **5a** bears a negative group charge, it has a small positive group charge in **5b** ( $q(\text{ring}) = 0.04$  (Mulliken) and 0.03 (NPA) at the B3LYP/6-31G(d) level; Figure 4).

The most fundamental change in zwitterionic intermediate **5c** ( $\mu = 20.9$  D, Figure 4) with respect to **5** is the enthalpic tradeoff of two O–H bonds for two weaker N–H bonds. It is the balance between alternating bond strengths and Coulombic destabilization due to charge separation that accounts for the net energy increase.<sup>15a</sup> When there are small changes in the relative positions of the heavy (nonhydrogen) atoms and no changes in their connectivity, the change in charge distribution due to proton transfer is minimal and in no way reflects the formal charges. The dipole moment of gas-phase **5c** has increased markedly relative to that of **5** ( $\Delta\mu = 15.1$  D, Figures 3 and 4). At the MP2/6-31G(d) level, putative GS reactant **5c**,

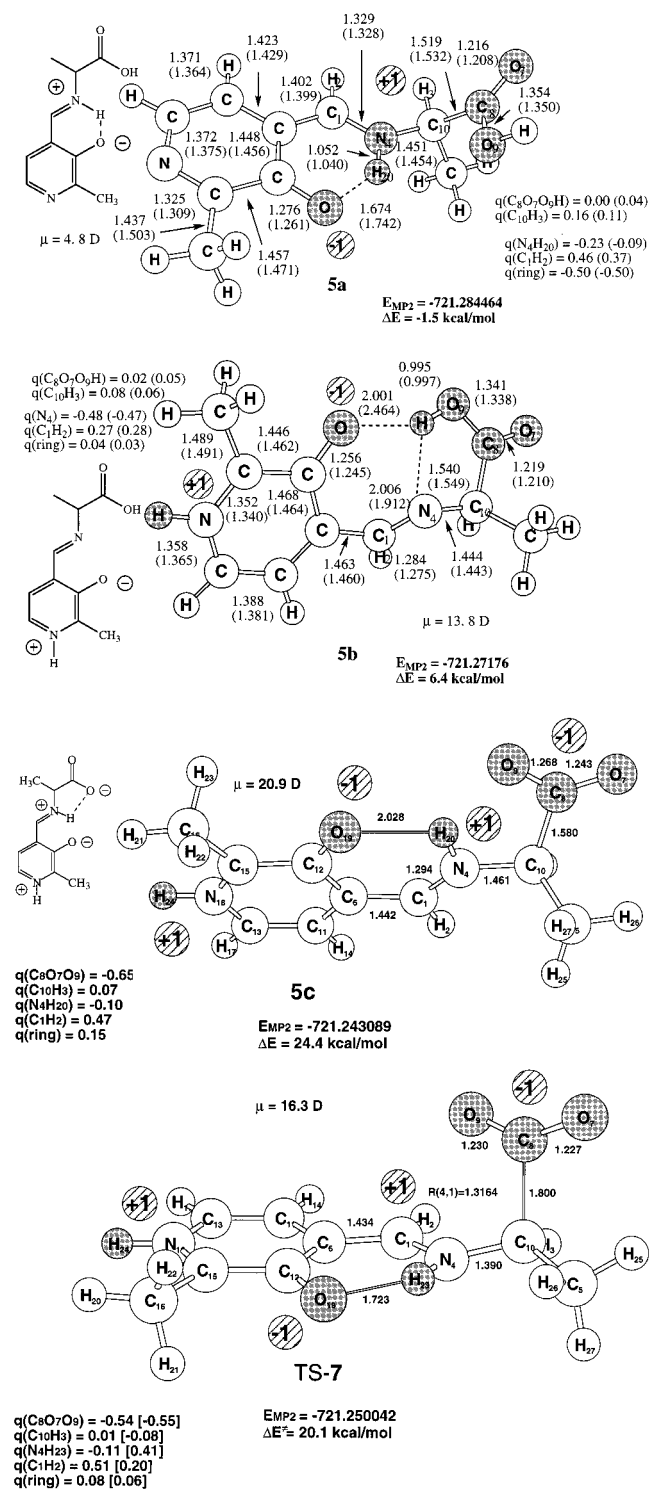


**Figure 4.** Alanine imine with PLP (structures **5a–c**) and the transition structure for decarboxylation (TS-7). The geometries are fully optimized at MP2/6-31G(d) and B3LYP/6-31G(d) (for **5a** and **5b**) levels. Energies are given in hartrees, distances in angstroms, and angles in degrees. MP2 relative energies are given with respect to **5**. Group Mulliken charges are given as  $q$ , and the net changes (for TS-7 with respect to **5**) are in square brackets. Geometrical parameters and NPA charges for **5a** and **5b** calculated at the B3LYP/6-31G(d) level are indicated in parentheses.

which is comparable in structure to intermediate **B** in Scheme 1, is 24.4 kcal/mol higher in energy than **5** and is, in fact, even higher in energy than TS-7 (see below). To assess the effect of Coulombic destabilization on the barrier for decarboxylation,

we must locate the TSs for decarboxylation that are related to these zwitterionic intermediates.

**(b) The Effect of Coulombic Destabilization on the Barrier for Decarboxylation.** We examined initially the effect of the pyridoxal ring on the overall barrier for decarboxylation. At the MP2/6-31G(d) level, the barrier height for the loss of  $\text{CO}_2$  from the simple imine model **1** (as in TS-2, Figure 1) is predicted to be 29.8 kcal/mol (Table 1). The barrier for decarboxylation of **5** was reduced to 22.0 kcal/mol (TS-6, Figure 3). This barrier is lower (16.1 kcal/mol) at the B3LYP/6-311G(d,p) level (however, a tendency of the B3LYP functional to underestimate activation barriers has been documented).<sup>13b,16</sup> The neutral phenolic oxygen is hydrogen bonded with the iminium hydrogen ( $R(\text{O}_{19}\text{H}_{23}) = 1.905 \text{ \AA}$ ) in TS-6. In this pathway, since the phenol is not ionized, the resulting charge-separated product of decarboxylation, intermediate **7**, remains fairly high in energy (15.6 kcal/mol). Thus, extension of the simplest model imine system with either the amide functionality in **3** or the pyridoxyl moiety in **5** (path A, Scheme 2) results in a further decrease in barrier height for decarboxylation of 6.7 and 7.8 kcal/mol, respectively. In both transition structures, the 1,4-proton shift to the imine nitrogen was complete before the barrier was crossed. For those reactions of a neutral carboxylic acid involving a 1,4-proton shift in concert with the loss of  $\text{CO}_2$ , it is the transferring of the proton to the imine nitrogen that neutralizes the putative negative charge arising from C–C bond cleavage.

We next considered decarboxylation via path B, involving zwitterion **5b**. Zwitterionic intermediate **5b** (Figure 4), which may be derived formally from **5** by intramolecular transfer of the phenolic proton, is 6.4 kcal/mol higher in energy than neutral structure **5** (Scheme 2). The transition structure for the decarboxylation of this species with multiple charge alternation (TS-7, path B) is only 20.1 kcal/mol above neutral structure **5** (Figure 4). As a consequence of the increase in the GS energy (6.4 kcal/mol), the activation barrier for the decarboxylation relative to the energy of zwitterion **5b** via TS-7 is reduced to 13.7 kcal/mol at the MP2/6-31G(d)/MP2/6-31G(d) level. If the relative energies of **5b** and TS-7 can be lowered at the active site as a consequence of complementary hydrogen bonding with neighboring residues, then the overall barrier would approach 13.7 kcal/mol and place this decarboxylation well within the desired range of 13–18 kcal/mol for efficient enzymatic reactions. The NPA charges calculated for **5b** at the B3LYP/6-31G(d) level (Figure 4) are close to the Mulliken charges calculated using the HF/6-31G(d) wave function and the MP2/6-31G(d) geometry. It should be noted that the charge distribution in TS-7 resembles closely intermediate **B** given in Scheme 1 for the generally accepted enzymatic decarboxylation process in PLP-dependent systems, emphasizing the importance of Coulombic destabilization in lowering the activation energy for the loss of  $\text{CO}_2$ .

The pathway for the decarboxylation of **5b** also resembles that of **3**, where a 1,4-hydrogen shift to nitrogen, affording the

(15) (a) The experimental gas-phase proton affinity (PA) of the phenoxy anion is 348.1 kcal/mol, and the PA of pyridine is only 222.3 kcal/mol, as a consequence of neutralization of charge upon acquiring a proton in the former and formation of a cation in the latter.<sup>15c</sup> At an infinite distance between charged centers, this electrostatic interaction results in a large energy increase that is reduced to about 6 kcal/mol when the charged centers are brought together as in **5b**. (c) Data from NIST Standard Reference Database 69, August 1997 Release: NIST Chemistry WebBook (<http://webbook.nist.gov/chemistry>).

(16) (a) Glukhovtsev, M. N.; Bach, R. D.; Pross, A.; Radom, L. *Chem. Phys. Lett.* **1996**, *260*, 558. (b) Bach, R. D.; Glukhovtsev, M. N.; Gonzalez, C.; Marquez, M.; Estevez, C. M.; Baboul, A. G.; Schlegel, H. B. *J. Phys. Chem. A* **1997**, *101*, 6092.

essential iminium ion functionality, precedes the loss of CO<sub>2</sub> (TS-4a and TS-4b). In a kinetic isotope effect (KIE) study on PLP-dependent histidine decarboxylase, Abell and O'Leary<sup>17</sup> found that the observed nitrogen KIE requires that the imine nitrogen in this Schiff base is protonated. In the systems that we have examined thus far that are neutral overall, either an adjacent positively charged ammonium<sup>13a</sup> or an iminium ion<sup>13b</sup> resulting from a proton shift is essential to the decarboxylation process. In both the  $\beta$ -keto acid<sup>13a</sup> and pyruvamide-dependent<sup>13b</sup> decarboxylation reactions, an intramolecular proton shift takes place from the carboxyl group to a neighboring carbonyl or imine group that provides a neutral leaving group. These observations raise the question of whether TS-7 is connected to **5b** and involves a 1,4-hydrogen shift as described above for TS-4 or if zwitterion **5c** is implicated. Since zwitterion **5c** is 4.3 kcal/mol higher in energy than TS-7 in the gas phase, the position of the equilibrium between intermediates **5b** and **5c** on the enzymatic pathway remains an open question. While the N $\cdots$ H–O hydrogen bond distance is 1.540 Å in **5b**, the O $\cdots$ H–N hydrogen bonding is presumably weaker in **5c** (1.817 Å). Both pathways take advantage of a protonated imine, but only the lower energy path **B** explicitly uses hydrogen bonding to the phenoxy anion (TS-7). The shorter O $\cdots$ H hydrogen bonding distance in TS-7 (1.723 Å, Figure 4), when compared with the O $\cdots$ H distance in TS-6 (1.905 Å, Figure 3), also serves to lower the activation barrier. The proton on the imine is the result of general acid catalysis by the phenol. This observation is further buttressed by animation of the normal modes of the single imaginary frequency (first-order saddle point) for TS-7, exhibiting a vibronic motion for H<sub>23</sub> between O<sub>19</sub> and N<sub>4</sub> in concert with the C–CO<sub>2</sub> bond stretch.

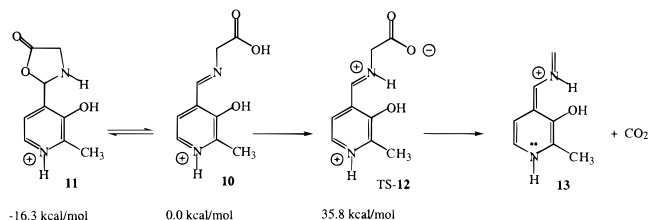
As a consequence, it might appear that **5c** is too high in energy to play a significant role as an intermediate in PLP-dependent enzymatic decarboxylations. Just as amino acids exist in polar media as zwitterions, energetically favorable interactions with the requisite amino acid residues at the active site could also significantly stabilize **5c**. Therefore, it is quite possible that Coulombic interactions of this dipolar species ( $\mu = 20.9$  D) with residues at the active site would reduce its energy to a point where a zwitterionic structure resembling **5c** could represent the GS configuration (intermediate **B**, Scheme 1) and proceed to TS-7 with a relatively low barrier. There is little question that path **B** is favored energetically over path **A** and that TS-7 is connected to quinonoid intermediate **8** and CO<sub>2</sub> and remains only 6 kcal/mol higher in energy than PLP model **5** (Scheme 2). The kinetic products (**8** + CO<sub>2</sub>) are slightly endothermic relative to **5**, but the overall decarboxylation process is exothermic, and the products (**9** + CO<sub>2</sub>) are 22.2 kcal/mol lower in energy than **5**.

The relative effects of solvation at the active site can be approximated as a continuum of uniform dielectric constant  $\epsilon$ , the reaction field. We have arbitrarily chosen a dielectric constant of 8 and used the self-consistent isodensity polarized continuum model (SCI-PCM)<sup>10</sup> to establish the trend for stabilization in the gas phase versus solution (Table 2). Intermediate **5a** (Scheme 2) is stabilized by 2.1 kcal/mol relative to neutral PLP model **5**, while the higher energy zwitterionic intermediate **5b** is increased in energy by 3.0 kcal/mol, despite its much higher dipole moment ( $\Delta\mu = 9.0$  D). More significantly, the relative energy barrier for the decarboxylation of **5**, TS-7, is reduced to 10.9 kcal/mol; a reduction of almost one-half as a consequence of this relatively nonpolar medium. The

**Table 2.** Single-Point SCI-PCM Calculations at the MP2/6-31G(d) Level (Dielectric Constant = 8)

compd	$E_{\text{total}}$	$E_{\text{rel}}$ (kcal/mol <sup>-1</sup> )
<b>5</b>	-721.295 687	0.00
<b>5a</b>	-721.299 027	-2.10
<b>5b</b>	-721.290 895	3.01
TS-7	-721.278 263	10.93

### Scheme 3



dipole moment of TS-7 ( $\Delta\mu = 16.3$  D) has realized a significant increase over that of neutral **5** but remains fairly close to that of **5b** ( $\Delta\mu = 13.8$  D) as a consequence of the greater charge separation. While it may be desirable to do a more extensive SCRF study on this process, problems with SCF convergence and cavity definition on systems this large suggest that a note of caution is in order and that such data should be taken as preliminary.

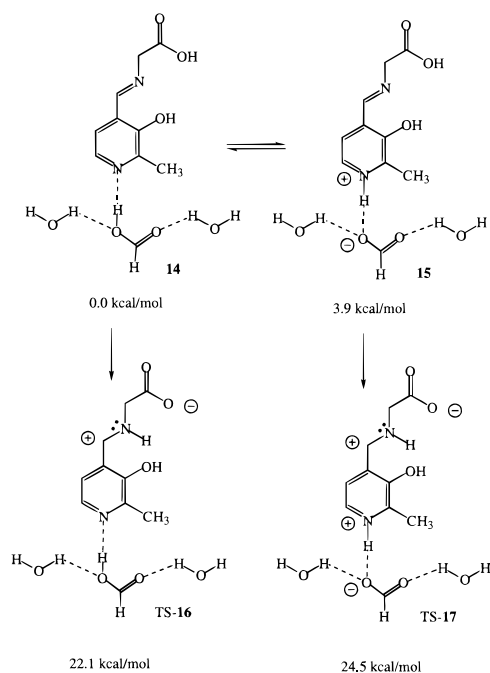
Thus, catalytic rate enhancement may be accomplished by destabilizing the GS or solvating the TS or both. Excessive destabilization due to the ionized groups of the PLP-bound substrate in the GS may cause the zwitterionic structure to revert to its neutral or un-ionized form, resulting in a loss of the essential charge separated structural features responsible for its electrostatic stabilization attending the loss of CO<sub>2</sub>. Although the cofactors in both pyruvoyl- and PLP-dependent decarboxylation processes make a meaningful contribution to the decarboxylation barriers (6.7 and 7.8 kcal/mol), the dominant factor in lowering the barrier height (based upon comparison with glycine and the simplest model **1**) remains the electrostatic stabilization provided by the adjacent positively charged iminium functionality in the transition state.<sup>13a,b</sup>

**3.4. Protonated PLP Model.** Next we addressed the question of how the barrier for the decarboxylation of **5** is affected by protonation of the pyridoxal nitrogen. Part of the mechanistic dogma surrounding this cofactor suggests that the electron pair derived from the C–COO<sup>-</sup> bond cleavage is delocalized into the PLP ring (intermediate **C**, Scheme 1), affording a quinonoid intermediate such as **8**, bearing a proton on nitrogen (Scheme 2). The simplest approximation is to protonate PLP model **5** and compute the reactant and transition structure for decarboxylation of the naked cation **10** (Scheme 3). As a consequence of the protonation of the pyridine ring, a stationary point with the carboxyl proton transferred to the imine nitrogen could not be located. The geometry optimization proceeded to the cyclic structure **11** that lies 16.3 kcal/mol below the open-chain minimum **10**.

At the HF/6-31G(d) level, the activation barrier for neutral TS-6 is 41.0 kcal/mol, and that for the loss of CO<sub>2</sub> from cation **10** to form cation **13** is 35.8 kcal/mol. Thus, we observe a lowering of the barrier ( $\Delta\Delta E^\ddagger = -5.2$  kcal/mol) at the HF level of theory relative to TS-6 (Scheme 2; the HF barriers are typically overestimated, see section 3.1). Nonetheless, this is still a relatively small decrease in the barrier height for the *unimolecular* decarboxylation of a cationic species. For example, fully protonated formylacetic acid has an activation barrier (MP2/6-31G\*) for decarboxylation only of 2.6 kcal/mol ( $\Delta\Delta E^\ddagger$

(17) (a) Abell, L. M.; O'Leary, M. H. *Biochemistry* **1988**, *27*, 5927. (b) O'Leary, M. H. *Acc. Chem. Res.* **1988**, *21*, 450.

## Scheme 4



= 25.9 kcal/mol).<sup>13a</sup> This trend stands in marked contrast to a reaction pathway involving a *bimolecular* gas-phase pre-reaction cluster, where the complexation energy of the pre-reaction GS complex is greater than that in the TS, as noted above. This prompted us to approximate more closely the environment at the active site, where conventional wisdom suggests that the pyridoxyl ring is protonated but the overall charge on the substrate is presumably negative (Scheme 1). Since TS-12 has a charge distribution comparable to that of TS-7, with the exception of the phenol hydrogen, we examined next the effect of a proton transfer to the nitrogen of the pyridoxal ring complexed to a solvated formate anion.

**3.5. PLP Model of the Active Site. (a) The Role of Aspartic Acid.** One of the many apparent functions of PLP is to “lock” the substrate into the active site. PLP-dependent enzymes (decarboxylases and amino-transferases) have been reported to accommodate the imine intermediate in a variety of hydrogen-bonded networks.<sup>17</sup> Crystal structures of dialkylglycine decarboxylase (DGD)<sup>18a</sup> show that the Asp243 carboxylate group is hydrogen bonded to two additional residues (His139 and Asn113) to impede its rotation. This is an unusual pyridoxal phosphate-dependent enzyme that catalyzes both decarboxylation and transamination. Heavy-atom kinetic isotope effects (KIEs) on  $k_{\text{cat}}$  show that the decarboxylation half-reaction largely limits the rate of the overall catalytic cycle of DGD.<sup>18b</sup> The observed <sup>13</sup>C KIE of 1.06 for a doubly labeled substrate suggests the presence of other partly rate-limiting steps. A solvent KIE of 1.6 indicates that a single proton is in flight in the TS. One possibility suggested was proton transfer to the pyridine nitrogen. In an attempt to establish more quantitatively the effect of protonation involving a counteranion (a salt bridge) on the barrier for loss of CO<sub>2</sub>, we allowed the model imine **5** to interact with formic acid and two water molecules (HCO<sub>2</sub>H·2H<sub>2</sub>O) according to Scheme 4.

The resulting hydrogen-bonding network is a model for the interaction of PLP with aspartic acid. Salt bridges are routinely

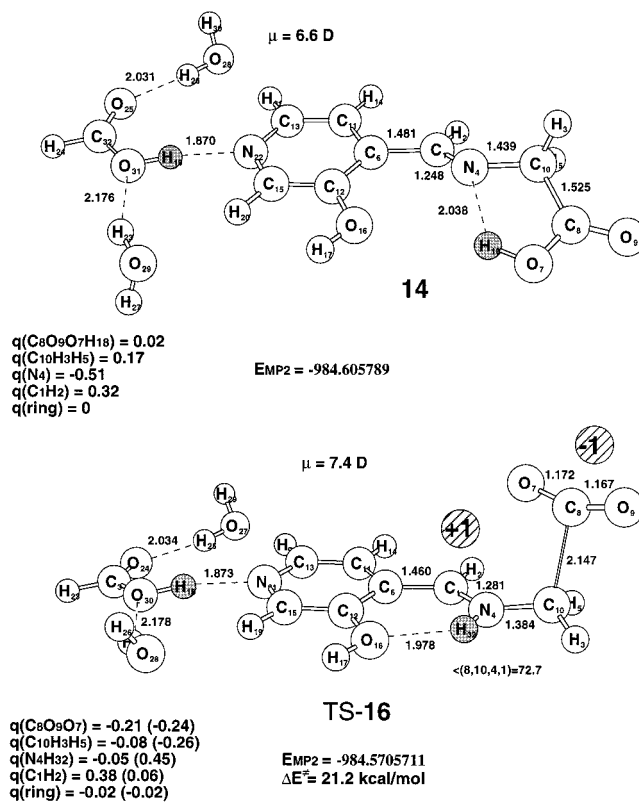


**Figure 5.** Glycine imine with PLP-neutral form (**14**) and its transition structure for decarboxylation (TS-16). The geometries are fully optimized at RHF/6-31G(d) level. MP2//HF/6-31G(d) energies are given in hartrees, distances in angstroms, and angles in degrees. Group Mulliken charges are given as  $q$  (the ring charge in **14** is assigned to zero as a reference charge), and net charges are in parentheses.

assumed to be in zwitterionic form. However, neutral form **14** (Figure 5) is the most stable complex, in the gas phase, at the MP2/6-31G(d)//HF/6-31G(d) level. The corresponding charged-separated structure **15** (Figure 6), where the proton has been transferred from formic acid to the ring nitrogen, lies 3.9 kcal/mol higher in energy, reflecting the modest influence of Coulombic destabilization. The position of the equilibrium is determined by the number and type of hydrogen-bonding interactions.<sup>13b</sup> In the absence of the two water molecules, a stationary point in the gas phase corresponding to proton transfer from formic acid to **5** does not exist. The decarboxylation of complex **15**, where the proton is fully transferred from formic acid to the PLP ring, had a higher barrier ( $\Delta E^\ddagger = 24.5 \text{ kcal/mol}$  with respect to **14**) than neutral PLP model **5** (TS-6) or PLP complexed to HCO<sub>2</sub>H·2H<sub>2</sub>O (TS-16, Figure 5) at the MP2/6-31G(d)//HF/6-31G(d) level of theory. If the barrier can be measured relative to **15**, as a result of GS stabilization of this dipolar intermediate, then this decarboxylation process would have a lower barrier than that for TS-6.

A compensating decrease in the energy of the surrounding microenvironment could potentially arise from complementary hydrogen-bonding interactions with residues adjacent to Asp243 (His139 and Asn113) that provide a stabilizing influence of comparable magnitude. In these two models, the phenol hydrogen is not directly involved in the enzyme catalysis, but the phenol oxygen is hydrogen bonded to the iminium hydrogen ( $R(\text{O}\cdots\text{H}) = 1.972 \text{ \AA}$ ). Hydrogen bonding of the phenol residue to an adjacent residue (Gln246) has been suggested.<sup>18a</sup> Thus, the barrier heights for decarboxylation with (TS-17, Figure 6) and without (TS-16) proton transfer to the pyridine nitrogen

(18) (a) Toney, M. D.; Hohenester, E.; Keller, J. W.; Jansoni, J. N. *J. Mol. Biol.* **1995**, *245*, 151. (b) Zhou, X.; Toney, M. D. *J. Am. Chem. Soc.* **1998**, *120*, 13282.



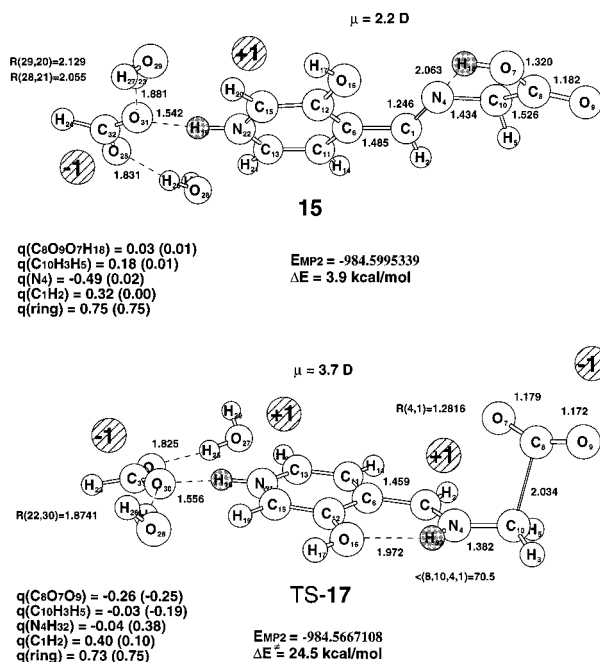


**Figure 6.** Glycine imine with PLP-zwitterionic form (**15**) and its transition structure for decarboxylation (TS-17). The geometries are fully optimized at RHF/6-31G(d). The MP2//HF/6-31G(d) energies are given in hartrees, distances in angstroms, and angles in degrees. Relative energies are given with respect to **14**. Group Mulliken charges are given as  $q$ , and the net changes from **14** are in parentheses.

relative to their respective reactant energies are comparable. The difference in the activation energies, although relatively small, ( $\Delta\Delta E^\ddagger = 2.4 \text{ kcal/mol}$ ) is due entirely to the electrostatic destabilization in zwitterionic reactant **15** relative to its neutral tautomer form **14** ( $\Delta E = 3.9 \text{ kcal/mol}$ ).

When the proton is transferred from the model Asp ( $\text{HCO}_2\text{H}\cdot 2\text{H}_2\text{O}$ ) to the pyridine nitrogen to form charge-separated but overall neutral complex **15** according to Scheme 4, the positive charge on the ring increases to 0.75. However, the change in the group charge on the pyridoxal ring on going from the ground to the transition state in both TS-16 and TS-17 is very slight (ca. 0.02). It has been generally accepted that the positively charged nitrogen of the pyridine ring acts as an electron sink to lower the free energy of C–H bond tautomerization or the loss of  $\text{CO}_2$ . Clearly, the latter function is not supported by our calculations on a system where the overall net charge is neutral.

A comparison of the activation barriers for decarboxylations of **14** and **15** via transition structures **16** and **17** (Figures 5 and 6), respectively, supports the conclusion above that proton transfer to the pyridoxyl ring has no influence on the rate of decarboxylation. Quinonoid intermediate **8** is 9.8 kcal/mol lower in energy than isomeric zwitterionic intermediate **8a** (Scheme 2). One function of proton transfer from Asp to the pyridinium nitrogen could be to raise the energy of the GS reactant and to stabilize intermediate **C** after the barrier is crossed (Scheme 1). The reaction pathway for PLP-dependent decarboxylation involving these zwitterionic tautomers has a lower activation barrier than that for the pathway in which the neutral reactant without charge separation undergoes decarboxylation (Figure 7).

**(b) The Role of the Arginine Residue.** Other groups in direct contact with the coenzyme at the DGD active site are the transamination catalytic base Lys272 and the hydrogen bond/salt bridge with Arg406.<sup>18a</sup> It is also thought that the phenolic group (presumably ionized) at position 3 enjoys a strong

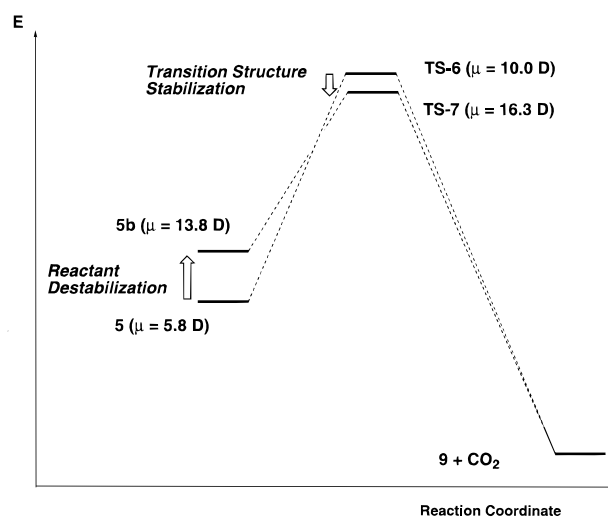


**Figure 7.** Qualitative scheme of ground-state destabilization and transition structure stabilization in PLP-dependent decarboxylation reactions. The relative energies calculated at the MP2/6-31G(d) level are given in Scheme 2.

hydrogen bond with the protonated aldimine nitrogen and also the side-chain amide nitrogen of Gln246. The carboxylate group accepts three hydrogen bonds in this model from Gln52, Arg406, and Lys272. These interactions, combined with the positive charge on Arg406 (and possibly Lys272), are thought to stabilize the ground state more than the TS for decarboxylation. The role of active residues at the active site cannot be modeled extensively, but a general trend can be established. For example, when TS-7 was extended to include a formamide molecule to model Gln246, the hydrogen-bonding interaction of the iminium hydrogen and phenoxy oxygen with the formamide  $\text{H}_2\text{NC}=\text{O}$  group resulted in an increase in the decarboxylation barrier of 4.4 kcal/mol, reflecting the decrease in the ground-state energy of the H-bonded pre-reaction gas-phase complex. This trend, reflecting an increase in the activation barrier, is typically what we observe when the GS stabilization is greater than that in the TS. The side-chain amide oxygen atom of Gln394 is also within hydrogen-bonding distance of the Arg406 guanidine group. The proximity of these residues presents an ideal opportunity for participation in a proton relay to dissipate the charge associated with the salt bridge prior to the loss of  $\text{CO}_2$ , as described below. The phosphate ester at position 5 is involved in a total of nine hydrogen bonds that we are unable to model.

An attempt to extend the theoretical model to include the aldimine portion of the active site was made by retaining the above structure with formic acid transferring a proton to the pyridine nitrogen as in **15** (Figure 6) and including a neutral guanidine accepting a proton from the carboxylic acid group of **15**. In a hydrophobic environment, the energy difference between the ionic salt and its neutral hydrogen-bonded complex is small, and the barrier that separates them is small. The ground-state energy of this ionic complex (**18**, Figure 8) is only 7.4 kcal/mol higher in energy at the HF/6-31G(d) level than the corresponding neutral hydrogen-bonded complex between **5**, formic acid $\cdot 2\text{H}_2\text{O}$ , and guanidine. It is notable that the group charge on the HN(pyridine) fragment is negative ( $-0.19$ ), in contrast to the positive formal charge. A formal charge of +1 is not localized on the guanidine cation (the group charge is only 0.17, Figure 8), while the group charge on the electronegative formate anion is  $-0.81$ . Inclusion of the guanidinium cation in hydrogen-bonded/salt-bridged reactant complex **18** ( $\mu = 17.6 \text{ D}$ ) resulted in a surprisingly large increase in the barrier

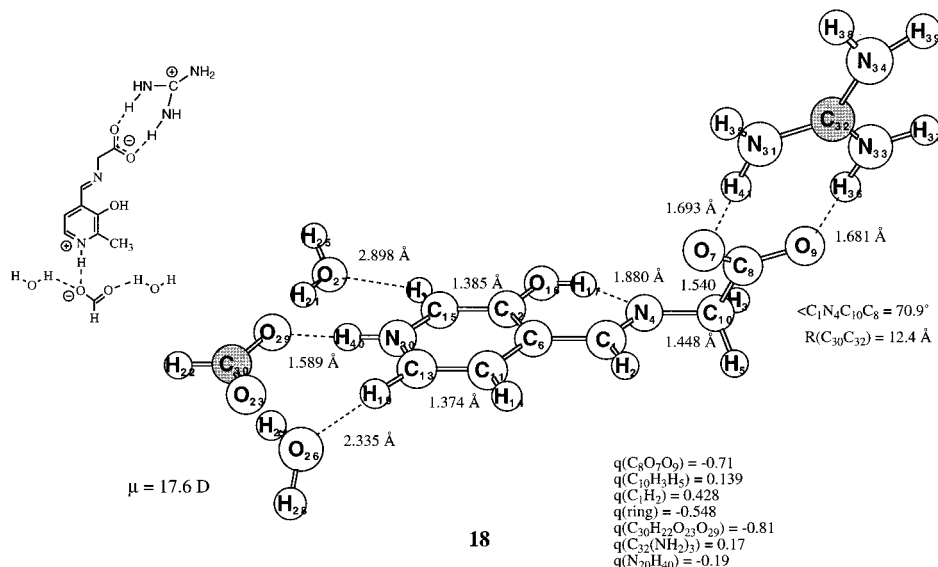


**Figure 8.** Glycine imine with PLP complexed to model aminoacid residues (**18**). The geometry was optimized at the RHF/6-31G(d) level ( $E_{\text{HF}} = -1186.04001$  hartrees). Mulliken group charges are given as  $q$ .

height for decarboxylation. Although a first-order saddle point was not located, when the forces on this TS were approaching the point of convergence, the total energy had increased by about 100 kcal/mol. At the HF level, the barrier for decarboxylation of **5** in its ionic form (TS-7) was 49.5 kcal/mol. Therefore, the dramatic increase in overall energy on going from the GS to the TS is due largely to the separation of charge attending the movement of  $\text{CO}_2$  that increases the distance ( $\approx 12$  Å) between the formate anion and guanidine cation (shaded atoms in **18**, Figure 8).

From these observations, we conclude that reactions such as decarboxylation, where the distance between oppositely charged particles is increased by the evolution of a neutral fragment ( $\text{CO}_2$ ), must proceed in a manner where the separation of charge in the microenvironment is diminished early along the reaction path. This can be achieved by a proton relay that annihilates the charge on the guanidine (salt bridge), accompanied by a proton transfer from the phenol to the imine nitrogen. An equivalent process could involve the concerted 1,4-proton shift from the neutral carboxylic acid to the imine nitrogen early along the reaction pathway (**5b**  $\rightarrow$  TS-7). We have seen this type of concerted proton transfer when pyruvate serves as the prosthetic group and the decarboxylation requires the presence of the protonated aldimine.<sup>13b</sup> Either pathway would be consistent with the solvent KIE, suggesting the transfer of a single proton in the rate-limiting step.<sup>18b</sup> From an evolutionary perspective, it would seem that the phenol should play a larger role than just hydrogen bonding, and direct involvement as a general acid catalyst to provide the obligatory positively charged iminium ion is suggested.

An earlier reported carbon KIE for the decarboxylation step of about 1.2 prompted the suggestion that the C–C bond is about two-thirds broken in the transition state.<sup>18a</sup> In TS-6 and TS-7, the C–C bond elongation is 19 and 14%, respectively. It has also been proposed that decarboxylation is catalyzed by stereoelectronic activation of the  $\text{C}^\alpha$ –carboxylate bond by its orientation perpendicular to the plane of the pyridinium ring.<sup>19</sup> This torsional angle in the GS of DGD has a value of  $\sim 35^\circ$  in both DGD- $\text{K}^+$  and DGD- $\text{Na}^+$ , reflecting the position of the Arg406 at the active site.<sup>18</sup> This dihedral angle in zwitterionic minimum **18** is  $70.9^\circ$  (Figure 8). Since the overlap of the breaking C–C bond with the adjacent  $\pi$ -system is a cosine

function, this angle would afford maximum  $\sigma$ – $\pi$  orbital overlap in the TS when this angle is  $\approx 90^\circ$ . It is then surprising that the  $\text{C}_8$ – $\text{C}_{10}$ – $\text{N}_4$ – $\text{C}_1$  dihedral angle in this series of TS varies from  $65.5$  to  $72.7^\circ$ .

In the present case, we suggest that the Arg406 salt bridge in minimum **18** is annihilated by a proton relay, presumably thermoneutral, from the Arg406 to a nearby base with rotation of the  $\text{C}^\alpha$ – $\text{CO}_2^-$  bond to a position where the anionic carboxylate group is nearly perpendicular to the plane of the PLP aromatic system. Consistent with this idea, the ratio of  $\beta$ -carboxylase/transaminase specificity of aspartate aminotransferase can be increased by  $6.5 \times 10^5$  by replacing the active-site Arg with alanine and introducing a new arginine residue nearby.<sup>9j</sup> As noted below, the localization of a negative charge on the carboxylate group serves to significantly lower the barrier for decarboxylation. In addition, the protein structural energy that would be required to reorient the dipolar groups so that they could accommodate the movement of the Arg406 residue to allow it to follow the developing  $\text{CO}_2$  fragment as the  $\text{C}_{10}$ – $\text{CO}_2$  distance increases would be excessive. When protonated guanidine (Arg406) remains in the plane of the PLP ring to stabilize the diminishing negative charge on the PLP residue as the partially negatively  $\text{CO}_2$  ( $\approx -0.5$  e) departs, the barrier rises sharply.

This leaves open the question of the purpose of the Arg406 residue at the active site. A viable possibility is that, prior to the base-catalyzed proton removal by Lys272 in the transamination step, the salt bridge<sup>20</sup> would revert back to its neutral form to facilitate proton removal adjacent to the  $-\text{COOH}$  group. An  $\alpha$ -C–H proton removal from a carboxylate anion has a high barrier. The neutral Arg406 residue would be required to hydrogen bond to the carboxylic acid, while general acid catalysis by the phenol to produce an iminium ion could Coulombically stabilize the TS for proton removal by Lys272.

**(c) The Influence of the Carboxylate Anion on the Activation Barrier.** We have shown that the activation barriers are reduced for unimolecular decarboxylation of a series of carboxylic acids in their anionic form. The increase in the ground-state energy associated with formation of a naked anion

(19) Dunathan, H. C. *Proc. Natl. Acad. Sci. U.S.A.* **1966**, *55*, 712.

(20) Zheng, Y.-J.; Ornstein, R. L. *J. Am. Chem. Soc.* **1996**, *118*, 11237.

due to deprotonation typically reduces gas-phase decarboxylation barriers by ca. 8–16 kcal/mol.<sup>13a,b</sup> A notable exception to this generalization is decarboxylation of *N*-carboxy biotin, where the loss of CO<sub>2</sub> is much faster from the neutral carboxylic acid as a consequence of a delocalized urea nitrogen anion leaving group.<sup>21</sup> Although electrostatic destabilization of the substrate carboxylate group can raise the energy of the ground state, the magnitude of this perturbation must not exceed the intrinsic activation energy for decarboxylation. A significant component of the  $\sim 10^9$ -fold increase that DGD provides over the nonenzymatic rate could be due to this ground-state destabilization. Formation of a carboxylate anion elevates the energy of the GS closer to that of the transition state and allows the enzyme to populate the conformation of the external aldimine intermediate in which the C <sup>$\alpha$</sup> –CO<sub>2</sub><sup>-</sup> bond is held nearly perpendicular to the PLP  $\pi$ -bonding iminium ion system. A recent crystal structure of a histidine decarboxylate–substrate analogue complex situates the carboxylate group in the crevasse lined with apolar residues.<sup>8c</sup> Such a medium supports the concept of electrostatic destabilization as a component of the catalytic mechanism, providing a potential mechanistic pathway whereby the substrate can gain sufficient internal energy to surmount the activation barrier.

The formation of the carboxylate anion of the substrate can be achieved either by a proton relay or by a 1,4-proton shift to the imine nitrogen in concert with the transfer of the phenolic hydrogen to an adjacent base (Gln246). In order for this to lower the barrier for decarboxylation relative to that of a neutral zwitterion, production of a localized carboxylate anion must be achieved in a nearly thermoneutral exchange of protons. The phenolic hydroxyl group is ideally located to provide either general-acid or -base catalysis in an intramolecular mode of action. To test this hypothesis, we calculated initially the energy for decarboxylation of the simplest naked PLP carboxylate anion **19**. The loss of CO<sub>2</sub> from **19**, affording anionic minimum **20**, is endothermic by 22.0 kcal/mol (Figure 9). The NH-tautomer of **20** (**20a**, 98) is 4.2 kcal/mol higher in energy than **20** (7.0 kcal/mol at the B3LYP/6-31G(d) level; see Table 3S in Supporting Information), although the O–H $\cdots$ N hydrogen bond distance is longer in **20** (1.726 Å) than the N–H $\cdots$ O hydrogen bond distance in **20a** (1.573 Å). The transition states for the decarboxylation of carboxylate anions such as **19** (the anionic equivalent of TS-6) are very difficult to locate and may actually be barrierless. We were able to estimate an activation energy of  $\approx 19$  kcal/mol (MP2/6-31G(d)) as the convergence limit was approached and the C–CO<sub>2</sub><sup>-</sup> bond distance reached 2.8 Å. As anticipated, the phenolic hydrogen is transferred to the imine nitrogen along the reaction coordinate to produce the necessary iminium ion moiety.

A potential enzymatic pathway could involve molecular motion, placing the C <sup>$\alpha$</sup> –CO<sub>2</sub><sup>-</sup> bond in conjugation with the PLP aromatic system, that is accompanied by general acid catalysis of the phenol hydrogen to form the protonated aldimine intermediate. To test this hypothesis, we have examined the energetics for decarboxylation of anion **19** complexed to neutral HCO<sub>2</sub>H $\cdot$ 2H<sub>2</sub>O. In this model, the proton is transferred from the phenol hydroxyl in minimum **21** to the imine nitrogen early along the reaction pathway to provide the electrostatic stabilization for TS-22 (Figure 10). This ground-state anionic structure **21** (Figure 10) is essentially neutral, but zwitterionic minimum **5c** (Figure 4) hydrogen-bonded to the formate anion (HCO<sub>2</sub><sup>-</sup>·2H<sub>2</sub>O<sup>-</sup>). The TS is equivalent to neutral TS-17 with the phenol

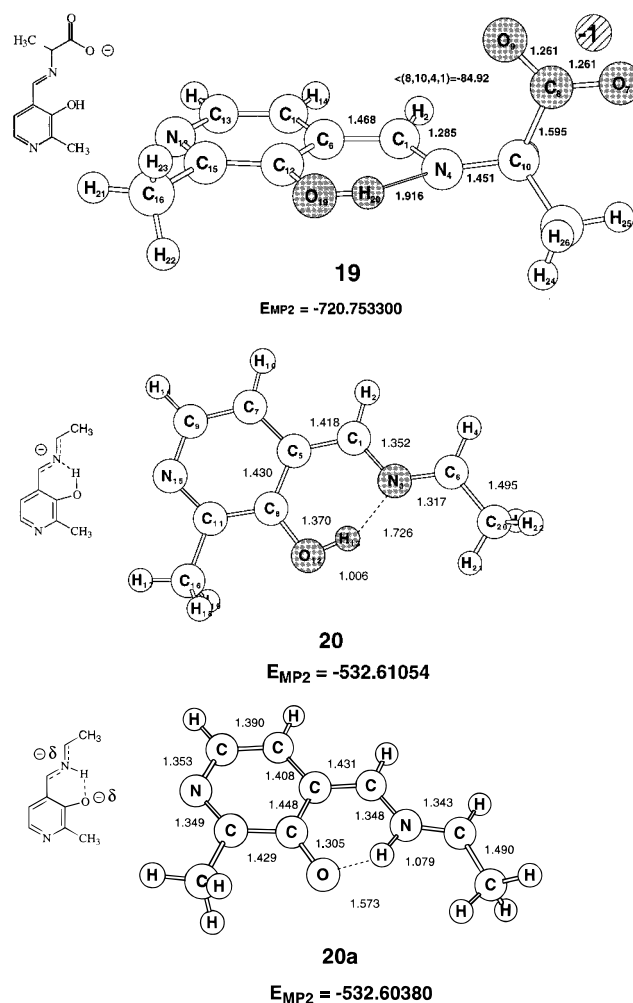


**Figure 9.** Carboxylate anion of the alanine imine of PLP (**19**) and the products of its decarboxylation (**20** and **20a**). The geometries are fully optimized at MP2/6-31G(d). Energies are given in hartrees, distances in angstroms, and angles in degrees.

hydrogen removed to produce an anionic transition state for decarboxylation.

The barrier height for the loss of CO<sub>2</sub> from anionic complex **21** at the HF/6-31G(d) level is 28.6 kcal/mol. The activation energy for decarboxylation of this carboxylate anion was reduced to 11.8 and 8.4 kcal/mol at the MP2//HF/6-31G(d) and B3LYP/6-311G(d,p)//HF/6-31G(d) levels. Geometry optimization at the B3LYP/6-31G(d) level until the forces (but not displacements) were converged gave a comparable classical barrier ( $\Delta E^\ddagger = 9.4$  kcal/mol). The lowering of the barrier height is a consequence of the increase in GS energy, the stabilizing influence of the short, strong hydrogen bond of the phenolic hydrogen ( $R(\text{O}–\text{H}) = 1.511$  Å), and the protonation of the pyridine nitrogen. These gas-phase barriers constitute a lower limit for decarboxylation of the carboxylate anion, since GS stabilization of this dipolar reactant at an active site would tend to increase the barrier height. However, the formation of an anionic cofactor is associated with an increase in energy that requires a compensating stabilization elsewhere in order for a net decrease in the barrier for decarboxylation.

When the TS bears an overall negative charge, protonation of the pyridine nitrogen has a significant impact upon the decarboxylation barrier ( $\Delta\Delta E^\ddagger \approx 10$  kcal/mol). The charge distribution in the PLP fragment of minimum **21** (Figure 10) shows the localization of a negative charge ( $-0.56$  e) on the CO<sub>2</sub> group, and this feature is quite similar to that in **5c** (Figure

(21) Bach, R. D.; Canepa, C.; Glukhovtsev, M. N. Unpublished results.

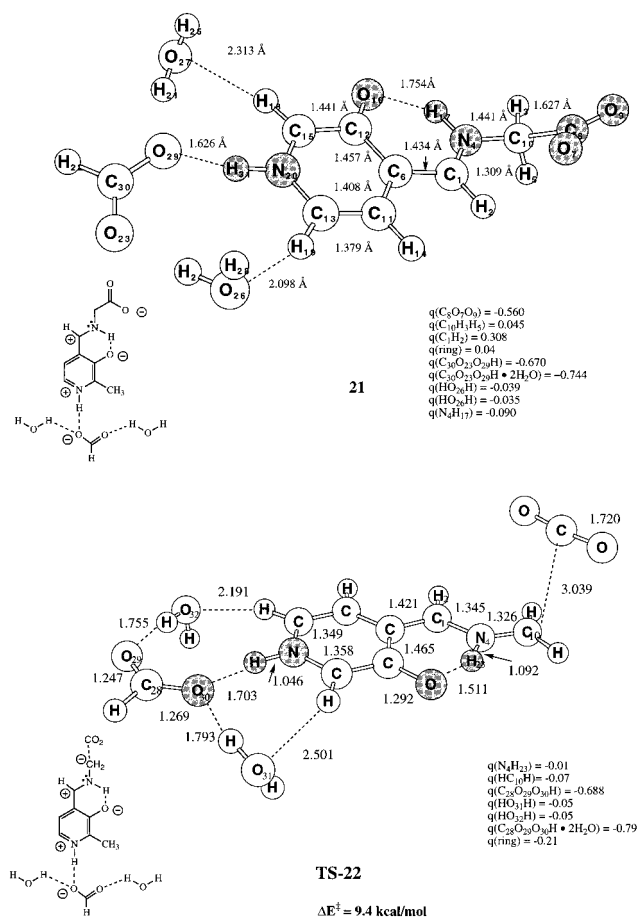


**Figure 10.** Glycine imine with PLP carboxylate anion **21** and its transition structure (TS-22) for  $\text{CO}_2$  elimination. The geometries were optimized at the B3LYP/6-31G(d) level (see the text for discussion of the optimization of **22**). Mulliken group charges are given as  $q$ .

4). It is notable that the  $\text{C}_{10}\text{--C}_8\text{OO}^-$  bond length in anion **21** is longer (1.627 Å) than those in minima **5b** (1.549 Å) and **5c** (1.580 Å) (Figure 4). This should facilitate the elimination of  $\text{CO}_2$ . The transfers of electron density from the formate anion complex to the PLP moieties in GS-**21** and TS-**22** are close to each other (0.25e and 0.21e). In contrast to TS-7, where the ring bears a positive charge (0.08) and the difference in the ring charges between the **5c** and TS-7 is only 0.06, the net ring charge in TS-**22** becomes negative (−0.21), whereas it is positive in minimum **21** (0.04) (Figure 10). The pyridine ring and the  $\text{HCO}_2 \cdot 2\text{H}_2\text{O}^-$  fragment combined bear essentially a full unit of negative charge (−0.79 e). A consequence of this charge redistribution is that the  $\text{N}\text{--H}\cdots\text{O}$  hydrogen bond (1.511 Å) becomes stronger in TS-**22** with respect to that in minimum **21** (1.754 Å), resulting in additional stabilization. This trend is quite opposite to the relative stabilization due to hydrogen bond formation that is observed for **5b**, **5c**, and TS-7. The  $\text{N}\text{--H}\cdots\text{O}$  hydrogen bond is presumed to be weaker in TS-7 (1.732 Å) than the  $\text{O}\text{--H}\cdots\text{N}$  hydrogen bond in **5b** (1.540 Å) or the  $\text{N}\text{--H}\cdots\text{O}$  hydrogen bond in **5c** (1.817 Å). Thus, anionic TS-**22** is stabilized with respect to reactant **21**, and this contributes to the lower activation barrier for  $\text{CO}_2$  elimination when compared with that for neutral TS-7. The major difference between the neutral and charged decarboxylation pathways, besides the fact that the latter process has a much lower barrier, is that the transition structure in the neutral case (e.g., TS-7) still maintains most of its initial charge on the carboxylate moiety, while the TS for an anionic system has essentially a neutral  $\text{CO}_2$  fragment (e.g., TS-**22**). The major conclusion to be drawn from this

section is that a localized negative charge on the PLP cofactor, however derived, will result in a lowering of the barrier for decarboxylation relative to the energy of the anionic GS.

**(d) An Analysis of the “Electron Sink” Concept.** In the classical rationalization of the role of the PLP aromatic system based upon the “electron sink” concept,<sup>9</sup> the extended conjugation of the developing charge on the  $\alpha$ -carbon into the  $\pi$ -electrons of the pyridine ring has been postulated according to Scheme 1. An inspection of the charge distributions in TS-2 and all related neutral structures involving the pyridine rings shows that the  $\text{CH}_2$  group charge at  $\text{C}^\alpha$  in the TSs remains essentially zero. The group charge on the pyridoxal ring is also essentially unchanged on going from **5** to TS-6 ( $\Delta q = 0.04$ ) (Figure 3). The reaction path for decarboxylation results in a negative carboxylate group ( $q = -0.54$ ) in TS-7, with a comparable amount of positive charge residing on the “benzylic”  $\text{C}\text{--H}$  ( $\text{C}_1\text{--H}_2$ ) group, where the group charge is 0.51 (Figure 4). Predictably, on the basis of electronegativity, the group charge on the  $\text{N}\text{--H}$  group ( $\text{N}_4\text{--H}_2$ ), where the nitrogen bears a formal charge of +1, is negative ( $q = -0.11$ ). Thus, the bulk of the positive charge resulting from 1,4-proton transfer actually resides on the  $\text{C}_1\text{--H}_2$  carbon–hydrogen fragment, thereby effectively neutralizing the negative charge associated with  $\text{C}\text{--C}$  bond cleavage and negating the presumed need to delocalize this charge into the pyridine ring. *The overall change in the pyridine group charge in TS-7 (Figure 4) is more positive (0.06) than that in the ground-state structure 5.* However, the charge distribution is not that anticipated on the basis of the electron distribution suggested by Scheme 1. In no case of neutral reactants have we seen a shift of electron density away from the potential developing carbanion at  $\text{C}^\alpha$ , as suggested by conventional wisdom. We do see the structural features associated with the proposed zwitterionic structures outlined in Scheme 1, but since *the anticipated charge distributions have been based upon formal charges*, we do not observe concurrence with what has typically been assumed by the experimental community.

However, in the decarboxylation of anionic complexes such as **21**, we have a unit of negative charge that must be dispersed over the remaining substrate in the TS after the loss of carbon dioxide. In the anionic transition structure, we typically find a relatively long carbon–carbon bond ( $\text{C}\text{--COO}^-$ ), which often makes it very difficult to locate a first-order saddle point for this endothermic process that quite possibly occurs without a barrier. Thus, the barrier is effectively the endothermicity of the reaction. A neutral  $\text{CO}_2$  fragment is essentially completely formed that requires that the negative charge in TS-**22** is delocalized over the pyridoxyl ring rather than remaining largely localized on the departing carboxylate group (Figure 10). Upon moving from GS-**21** to TS-**22**, we observe a net change in charge of the pyridine ring (including its substituents) of −0.25 e, consistent with the basic premise of the electron sink effect but for an entirely different reason. The decarboxylation of anionic systems tends to be endothermic in nature. An anionic decarboxylation reaction is associated with a very late TS, which requires that the negative charge be localized over a smaller number of atoms of lesser electronegativity. While most of the TSs for decarboxylation that we have described involve a Coulombically stabilized carboxylate, if the formation of an essentially localized naked carboxylate anion can be achieved without a large expenditure of energy, then there is little question that this would provide an efficient enzymatic decarboxylation pathway.

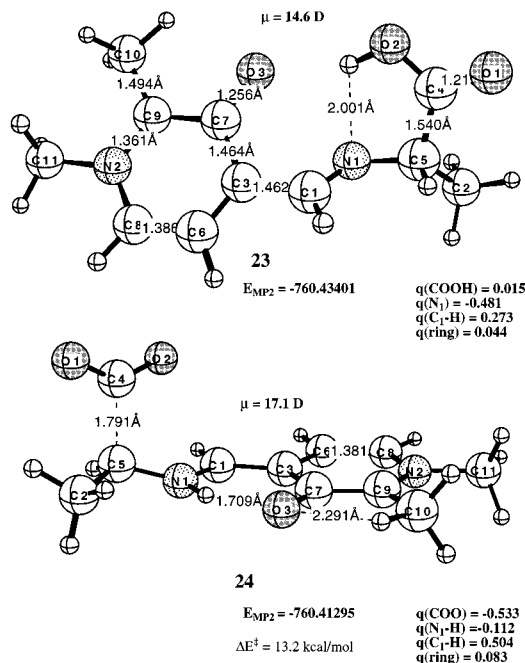


**Figure 11.** *N*-Methyl-PLP model **23** and its transition structure for decarboxylation, TS-**24**. The geometries were fully optimized at MP2/6-31G(d). Energies are given in Hartrees, distances in angstroms, and angles in degrees.

The idea of moving an electron pair from the breaking C—C bond to the pyridine nitrogen is aesthetically very pleasing, but the separation of charge attending movement of electrons in such a manner requires work. A classic experiment to prove the electron sink concept has typically been to utilize *N*-methyl-PLP, where it was assumed that “the ring nitrogen has a permanent positive charge”. Recent experimental studies in support of the electron sink effect, where the cofactor analogue *N*-methyl-PLP was employed in an effort to get a full positive charge on the pyridine ring, shows a modest 10-fold recovery of enzymatic activity.<sup>22a</sup> While it has been suggested that the negative charge of ASP stabilizes the positive charge at N(1) that accelerates abstraction of the  $\alpha$ -proton from the amino acid substrate,<sup>22b,c</sup> the observation of a quinonoid intermediate in aminotransferase reactions is not necessarily consistent with a rate enhancement resulting from transfer of electron density to the pyridine ring. As suggested above in our decarboxylation studies, the function of the proton (or methyl group) on the pyridine nitrogen could be to stabilize such a quinonoid intermediate (Scheme 2), making its observation spectroscopically more likely.

We have examined the influence of *N*-methyl-PLP on the barrier for decarboxylation using the *N*-methyl derivatives corresponding to TS-**6** and TS-**7**. The neutral *N*-methyl-PLP ground state, **23** (Figure 11), is a zwitterionic structure with a formal negative charge on the ring oxygen and a formal positive charge on the pyridine nitrogen corresponding to ground-state minimum **5b** (path B, Scheme 2). The calculated charges on oxygen and nitrogen are  $-0.734$  and  $-0.600$ , respectively. The barrier for decarboxylation of **23** (TS-**24**,  $\Delta E^\ddagger = 13.2$  kcal/mol, Figure 11) is essentially the same as that of TS-**7** (13.7 kcal/mol), showing that the *N*-methyl group does not influence the decarboxylation barrier any more than the proton on nitrogen.

(22) (a) Gong, J.; Hunter, G. A.; Ferreira, G. C. *Biochemistry* **1998**, *37*, 3509. (b) Yano, Y.; Hinoue, Y.; Chen, V. J.; Metzler, D. E.; Miyahara, I.; Hirotsu, K.; Kagamiyama, H. *J. Mol. Biol.* **1993**, *234*, 1218. (c) Yano, T.; Kuramitsu, S.; Tanase, S.; Morino, Y.; Kagamiyama, H. *Biochemistry* **1992**, *31*, 5878.

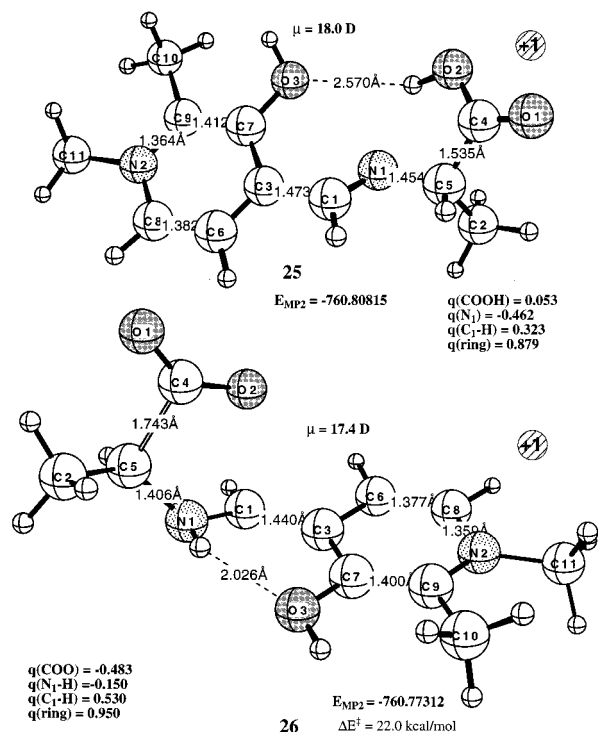


**Figure 12.** *N*-Methyl-PLP model cation **25** and its transition structure for decarboxylation, TS-**26**. The geometries were fully optimized at MP2/6-31G(d). Energies are given in hartrees, distances in angstroms, and angles in degrees.

The charge on the ring in neutral GS-**23** is 0.043, while that in TS-**24** is slightly more positive (0.082), consistent with the charge distribution in the *N*-protonated structures in Scheme 2. The charge on the pyridine nitrogen is  $-0.616$  in TS-**24**, while that on the *N*-methyl group is 0.35.

We have also examined the effect of a full positive charge on the pyridine ring on the decarboxylation barrier. The positively charged *N*-methyl-PLP minimum **25** (Figure 12), having a proton on the phenol oxygen, has a net charge on the ring of 0.88. This charge *increases* to 0.95 in TS-**26** (Figure 12), and the barrier for decarboxylation also *increases* to 22.0 kcal/mol. Thus, *we see no evidence for an increase in the rate of decarboxylation due to a positively charged pyridine ring or to a positively charged amide group (TS-4b).*

#### 4. Conclusions

(1) The barrier for the decarboxylation of the simplest imine **1** ( $\text{H}_2\text{C}=\text{N}=\text{CH}_2-\text{COOH}$ ) is 29.8 kcal/mol. Inclusion of the 2-hydroxy-3-methylpyridine group, as in **5**, results in a decrease in barrier height to 20.1 kcal/mol. The lower activation barrier for neutral TS-**7** is attributed to delocalization of positive charge at the adjacent C—H group.

(2) Either an intramolecular 1,4-proton shift from the carboxylic acid group or general acid catalysis by the phenol group in **5** affords a protonated aldimine group that provides Coulombic stabilization for the decarboxylation step (TS-**6** and TS-**7**).

(3) The “electron sink” effect attributed to the amide functionality in pyruvoyl-dependent and the pyridoxyl group in PLP-dependent decarboxylation is absent for neutral and/or zwitterionic substrates. There is no change in electron density of the pyridoxyl ring in either transition structure (TS-**6** or TS-**7**). The barrier heights of the pyruvoyl-dependent (TS-**4**) and PLP-dependent (TS-**7**) decarboxylations are quite similar. Thus,

nature has evolved two equally efficient processes for the catalysis of decarboxylation, and neither of them appears to be driven by the accepted paradigm of electron delocalization through an "electron sink" mechanism. These theoretical data suggest that the primary function of proton transfer from Asp to the pyridinium nitrogen appears to be to raise the energy of the GS reactant and to stabilize intermediate C after the barrier is crossed (Scheme 1).

(4) In reactions involving salt bridges, either the potential for an increase in distance between oppositely charged centers must be alleviated early along the reaction coordinate by annihilation of the salt bridge, or structural rearrangement of the protein must allow the neutral CO<sub>2</sub> to escape in order to avoid marked increases in energy.

(5) The barriers for decarboxylation reactions of systems bearing a net negative charge are about 10 kcal/mol lower than their corresponding neutral and/or zwitterionic counterparts. The formation of a localized carboxylate anion represents a highly efficient pathway for the decarboxylation step.

(6) The energy gap between the ground and transition states for PLP-dependent decarboxylation is reduced by the increase in energy of zwitterionic reactant intermediates and increased stabilization of these multiply charged intermediates in the transition state for decarboxylation.

(7) *N*-Methyl-PLP cofactors in either a neutral (zwitterionic) or a positively charged state have no influence on the barriers for decarboxylation and plays no role as an "electron sink".

## 5. Summary

The three pertinent structural features essential to efficient PLP-dependent decarboxylation are (i) the Coulombic influence of the protonated aldimine, (ii) the short, strong stabilizing hydrogen bond of the phenol oxygen anion with the imine hydrogen in the transition structure, and (iii) the formation of zwitterionic intermediates along the reaction coordinate with energy compensating Coulombic interactions of the charge-separated PLP cofactor with the amino acid residues at the active

site. The successful conversion of neutral reactant **5** to its tautomeric forms **5a–c** results in an increase in their dipole moments (from 5.8 to 20.9 D). Although the relative energies of these zwitterionic structures are higher than that of the neutral reactant and they exemplify, thereby, reactant destabilization, the surrounding active site environment can lead to a corresponding increase in stabilizing electrostatic interactions that lower energies of both zwitterionic reactants and transition structures. The reaction pathway for PLP-dependent decarboxylation involving these zwitterionic tautomers has a lower activation barrier than the pathway in which the neutral reactant undergoes decarboxylation. A proton relay or comparable process that generates a neutral but zwitterionic transition state such as TS-7 in a medium of low dielectric constant will dramatically lower the activation barrier for decarboxylation. Perhaps it is not too surprising that both pyruvoyl- and PLP-dependent decarboxylation processes have the same turnover number and operate at comparable rates by similar mechanisms having distinct rate-determining steps.<sup>9</sup> These data, taken collectively, suggest that another fundamental role of the pyridoxyl ring in the overall decarboxylation process is to provide a zwitterionic tautomer of the substrate as a consequence of general acid catalysis that diminishes the energy gap between the ground-state structure and the transition structure for decarboxylation.

**Acknowledgment.** This work was supported by the National Science Foundation (CHE-9696216). We are also thankful to the National Center for Supercomputing Applications (Urbana, IL) for generous amounts of computer time.

**Supporting Information Available:** Tables of total energies of **1**, **4–7** calculated at various levels of theory; total energies of **5**, **5a**, **5b**, and anions **20** and **20a** calculated at the B3LYP/6-31G(d) level (PDF). This material is available free of charge via the Internet at <http://pubs.acs.org>.

JA9907616